Quantum and Classical Mode Softening Near the Charge-Density-Wave–Superconductor Transition of Cu_xTiSe_2

H. Barath,[1] M. Kim,[1] J. F. Karpus,[1] S. L. Cooper,[1] P. Abbamonte,[1] E. Fradkin,[1] E. Morosan,[2] and R. J. Cava[2]
[1]*Department of Physics and Frederick Seitz Materials Research Laboratory, University of Illinois, Urbana, Illinois 61801, USA*
[2]*Department of Chemistry, Princeton University, Princeton, New Jersey 08544, USA*
(Received 17 September 2007; published 12 March 2008)

Temperature- and x-dependent Raman scattering studies of the charge-density-wave (CDW) amplitude modes in Cu_xTiSe_2 show that the amplitude mode frequency ω_0 exhibits identical power-law scaling with the reduced temperature T/T_{CDW} and the reduced Cu content x/x_c, i.e., $\omega_0 \sim (1-p)^{0.15}$ for $p = T/T_{CDW}$ or x/x_c, suggesting that mode softening is independent of the control parameter used to approach the CDW transition. We provide evidence that x-dependent mode softening in Cu_xTiSe_2 is associated with the reduction of the electron-phonon coupling constant, and that x-dependent "quantum" ($T \sim 0$) mode softening suggests the presence of a quantum critical point within the superconductor phase of Cu_xTiSe_2.

DOI: 10.1103/PhysRevLett.100.106402 PACS numbers: 71.45.Lr, 73.43.Nq, 74.70.−b, 78.30.−j

One of the most important current goals of condensed matter physics research involves elucidating the competition between diverse and exotic phases in strongly correlated matter, such as antiferromagnetism and superconductivity (SC) in the high T_c cuprates [1], heavy fermions [2], and cobaltates [3], and charge-density-wave (CDW) order and SC in materials such as Na_xTaS_2 [4]. Recently, Morosan *et al.* discovered an interesting new material exhibiting a competition between CDW order and SC: copper intercalated 1T-$TiSe_2$, i.e., Cu_xTiSe_2 [5]. 1T-$TiSe_2$ is a semimetal or small-gap semiconductor in the normal state [6–9], which develops a commensurate CDW with a $2a_0 \times 2a_0 \times 2c_0$ superlattice structure at temperatures below a second-order phase transition at $T_{CDW} \sim 200$ K [6,10]. Increasing Cu intercalation in $TiSe_2$ (increasing x in Cu_xTiSe_2) results in (i) an expansion of the a- and c-axis lattice parameters [5], (ii) increased electronic density of states near the L point [7,8], (iii) a suppression of the CDW transition temperature [5], and (iv) the emergence near $x = 0.04$ of an SC phase having a maximum T_c of 4.15 K at $x = 0.08$ [5].

The Cu_xTiSe_2 system provides an ideal opportunity to investigate the microscopic details of quantum ($T \sim 0$) phase transitions between CDW order and SC. It is of particular interest to clarify the nature of the "soft mode" in CDW-SC transitions: the behavior of the soft mode—i.e., the phonon mode whose frequency tends towards zero at the second-order phase transition—is one of the most fundamental and well-studied phenomena associated with classical (thermally driven) displacive phase transitions [11]; on the other hand, soft mode behavior associated with quantum phase transitions is not well understood. In this investigation, we use Raman scattering to study the temperature- and doping-dependent evolution of the CDW "amplitude" modes in Cu_xTiSe_2. The CDW amplitude mode [12]—which is associated with collective transverse fluctuations of the CDW order parameter—offers detailed information regarding the evolution and stability of the CDW state and the CDW soft mode. In this Letter, we show that the amplitude mode frequency in Cu_xTiSe_2 exhibits identical power-law scaling with the reduced temperature, T/T_{CDW}, and the reduced Cu content, x/x_c, indicating that mode softening in Cu_xTiSe_2 is independent of the control parameter used to approach the CDW transition, and we show that "quantum" ($T \sim 0$) softening of the CDW amplitude mode is consistent with a quantum critical point hidden in the superconductor phase of Cu_xTiSe_2.

Raman scattering measurements were performed on high quality single-crystal and pressed-pellet samples of Cu_xTiSe_2 for $x = 0$, 0.01, 0.02, 0.03, 0.04, 0.05, and 0.06, which were grown and characterized as described previously [5,13]. Figure 1(a) shows the $T = 6$ K Raman spectra of Cu_xTiSe_2 for various Cu concentrations (x). The $T = 6$ K Raman spectrum of $TiSe_2$ (top spectrum in Fig. 1) exhibits several spectroscopic features that have been reported previously [14,15], including a Raman-active $\mathbf{k} = 0$ phonon mode near 137 cm^{-1} that shows little change in energy (∼0.7%) and linewidth with increasing x. Figure 1(a) also shows several modes that appear below the CDW transition, including an A_{1g}-symmetry amplitude mode near 118 cm^{-1}, which arises from fluctuations of the CDW amplitude that preserve the ground state $2 \times 2 \times 2$ CDW structure, and an E_g-symmetry amplitude mode near 79 cm^{-1} [14,15]. These CDW amplitude modes are associated with the soft zone boundary TA phonon at the L-point [14,15], which is folded to the zone center when the unit cell is doubled below T_{CDW} [16].

Figure 2 summarizes the A_{1g} amplitude mode frequency (squares) and linewidth (circles) in Cu_xTiSe_2 as functions of (a) Cu concentration, x (for $T = 6$ K) and (b) temperature (for $x = 0$). The A_{1g} amplitude mode frequency and linewidth data were extracted from Lorentzian fits to the data, as illustrated in Fig. 1. Because the A_{1g} amplitude mode is in most cases well-separated from nearby optical modes, estimated errors in the amplitude mode frequency obtained in this manner were ≤1%. Figure 2(b) illustrates

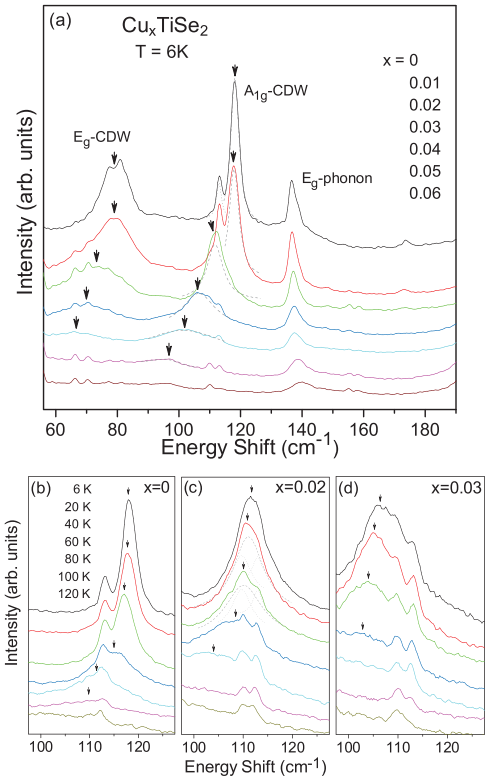

FIG. 1 (color). (a) Doping (x) dependence of the Raman spectrum of Cu$_x$TiSe$_2$ at $T = 6$ K, illustrating the E_g- and A_{1g}-symmetry CDW amplitude modes (arrows) as a function of x. (b)–(d) Temperature dependence of the A_{1g}-symmetry CDW mode spectra at (b) $x = 0$, (c) $x = 0.02$, and (d) $x = 0.03$ in Cu$_x$TiSe$_2$. The spectra have been offset for clarity, and the vertical scales in (c) and (d) are respectively 3× and 4× the vertical scale in (b). Also shown are example Lorentzian fits to the A_{1g} amplitude mode (dashed line) and nearby optical modes (dotted line).

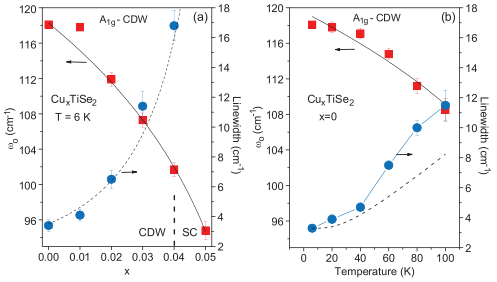

FIG. 2 (color). (a) Summary of the $T = 6$ K A_{1g}-symmetry CDW mode frequency (ω_0) vs x (filled squares) and the $T = 6$ K A_{1g}-symmetry CDW mode linewidth (FWHM) vs x (filled circles) for Cu$_x$TiSe$_2$. The solid line is a fit to the doping dependence of the $T = 6$ K frequency data using $\omega_0/\omega_0(0) = (1 - x/x_c)^\beta$ with $\beta \sim 0.15$ and $x_c \sim 0.07$, and the dashed line is a fit to $\Gamma \sim (x_c - x)^{-2}$ with $x_c \sim 0.07$. (b) Summary of the $x = 0$ A_{1g}-symmetry CDW mode frequency (ω_0) vs temperature (filled squares) and the $x = 0$ A_{1g}-symmetry CDW mode linewidth (FWHM) vs temperature (filled circles) for TiSe$_2$. The solid line is a fit to the frequency data with $\omega_0/\omega_0(0) = (1 - T/T_{\mathrm{CDW}})^\beta$ with $\beta \sim 0.15$. The dashed line illustrates the contribution to the linewidth expected from two-phonon damping. The estimated errors from the Lorentzian fits are $\leq 1\%$ for the frequency data and $\leq 8\%$ for the linewidth data.

that the A_{1g} amplitude mode of Cu$_x$TiSe$_2$ exhibits temperature-dependent soft mode behavior typical of amplitude modes observed in other CDW systems [17,18], including (i) a frequency with a power-law temperature dependence $\omega_0(T) \sim (1 - T/T_{\mathrm{CDW}})^\beta$ with $\beta \sim 0.15$ [solid line, Fig. 2(b)], (ii) a weakening of the amplitude mode intensity as the CDW lattice loses coherence as $T \rightarrow T_{\mathrm{CDW}}$, and (iii) a dramatic increase in linewidth with increasing temperature; the latter mainly reflects overdamping of the amplitude mode due to an increase in CDW fluctuations, as it is in substantial excess of the broadening expected from anharmonic (i.e., two-phonon) contributions [dashed line, Fig. 2(b)].

Significantly, Fig. 1(a) shows that both the 79 cm^{-1} E_g and 118 cm^{-1} A_{1g} amplitude modes in Cu$_x$TiSe$_2$ also exhibit x-dependent mode softening that has nearly identical characteristics to temperature-dependent mode softening in Cu$_x$TiSe$_2$. For example, Fig. 2(a) shows that the A_{1g} amplitude mode softens by ~18% between $x = 0$ and $x = 0.05$ at $T = 6$ K (solid squares), and exhibits a 400% increase in linewidth between $x = 0$ and $x = 0.04$ at $T = 6$ K (solid circles). The dramatic x-dependent increase in the $T = 6$ K amplitude mode linewidths [filled circles, Fig. 2(a)] cannot be attributed to the effects of disorder, as there is not a comparably large increase in the other phonon linewidths with increasing x. Rather, x-dependent damping of the CDW amplitude modes in Cu$_x$TiSe$_2$ reflects a dramatic enhancement of CDW fluctuations—and a loss of CDW coherence—with increasing x. A microscopic analysis of the nature and origin of x-dependent mode softening in Cu$_x$TiSe$_2$ [see Fig. 2(a)] can be made using Rice and collaborators' mean-field result for the frequency of a CDW amplitude mode [12],

$$\omega_0 = 1.4\lambda^{1/2}\tilde{\omega}t^{1/2}, \qquad (1)$$

which has been successfully applied to the analysis of CDW soft mode behavior in other dichalcogenides [17]. In Eq. (1), $\tilde{\omega}$ is the unscreened (high temperature) phonon frequency, $t = (T_{\mathrm{CDW}} - T)/T_{\mathrm{CDW}}$ is the reduced temperature, and $\lambda = N(0)g^2(0)/\tilde{\omega}$ is the electron-phonon coupling constant associated with the CDW, where $g(0)$ is the electron-phonon coupling matrix element between the soft mode phonon and the electronic states at the Fermi surface involved in the CDW transition, and $N(0)$ is the joint density of states of the electrons and holes involved in the CDW transition [17]. Note that the unscreened frequency $\tilde{\omega}$ in Eq. (1) is not expected to have a significant doping dependence between $x = 0$ and $x = 0.06$ in Cu$_x$TiSe$_2$, which is supported by the fact that the optical phonon frequencies exhibit a negligible change with x. Consequently, Eq. (1) suggests that the x-dependent softening of the A_{1g} amplitude mode is associated with a

substantial reduction in the electron-phonon coupling constant λ with x in Cu_xTiSe_2. One possible source of this reduction is a decreased density of electrons/holes participating in the CDW transition between $x = 0$ and $x = 0.05$ in Cu_xTiSe_2, $N(0)$. Indeed, Morosan *et al.* observed a $\sim$50% decrease in the size of the magnetic susceptibility drop below T_{CDW} between $x = 0$ and $x = 0.05$ in Cu_xTiSe_2, indicating that fewer electronic states are gapped at the CDW transition with increasing x [5]. However, this reduction in $N(0)$ is not likely associated with a loss of Fermi surface nesting because ARPES studies of Cu_xTiSe_2 have shown that nesting actually increases with x [7]. Another possibility is that the linear expansion of the a-axis parameter with x in Cu_xTiSe_2 [5] leads to a reduction in λ by expanding the Ti-Se bond length primarily responsible for the CDW instability in $1T$-$TiSe_2$ [6,16,19]. This alternative is consistent with Castro Neto's proposal that the layered dichalcogenides have a critical lattice spacing above which CDW order is suppressed [20].

Remarkably, Fig. 3 shows that x-dependent and thermal mode softening in Cu_xTiSe_2 exhibit essentially identical scaling behavior. In particular, Fig. 3 compares the following data sets: (i) the normalized A_{1g} amplitude mode frequency $\omega_0/\omega_0(0)$ vs the reduced concentration x/x_c for $T = 60$ K (using $x_c = 0.06$ from Ref. [5]) (filled squares); and (ii) the normalized A_{1g} amplitude mode frequency $\omega_0/\omega_0(0)$ vs the reduced temperature T/T_{CDW} for $x = 0$ (using $T_{CDW} = 218$ K from Ref. [5]) (filled circles), $x = 0.02$ ($T_{CDW} = 180$ K [5]) (open triangles), and $x = 0.03$ ($T_{CDW} = 140$ K [5]) (open diamonds). The solid line in Fig. 3 shows that all these data sets collapse onto the same curve given by $\omega_0/\omega_0(0) = (1 - p)^\beta$, with $p = x/x_c$ or T/T_{CDW} and $\beta \sim 0.15$. An estimated uncertainty of $\Delta\beta = \pm 0.05$ in the "best fit" value of $\beta \sim 0.15$ is suggested by the gray lines in Fig. 3, which show the functional form $\omega_0/\omega_0(0) = (1 - p)^\beta$ for both $\beta = 0.20$ (bottom gray line) and $\beta = 0.10$ (top gray line).

Two key points should be made regarding Fig. 3: First, while we cannot measure the amplitude mode frequency with temperature (x) all the way to the critical point T_{CDW} (x_c), we can nevertheless extract a reliable value for the scaling parameter β from fits to these data because we know the values of T_{CDW} (for all x) and x_c (at $T = 60$ K) from Ref. [5]. Second, the scaling parameter $\beta \sim 0.15$ obtained from our amplitude mode data is substantially smaller than the value of $1/2$ suggested by the mean-field model of Eq. (1) [12]. However, the scaling parameter $\beta \sim 0.15$ in Cu_xTiSe_2 is consistent with the critical exponent for the order parameter in the 2D three-state Potts model, $\beta = 0.133$ [21]; this model is appropriate for the CDW in layered Cu_xTiSe_2 because of the three-fold degenerate CDW ground state in this material [6,11].

The "universal" scaling of the Cu_xTiSe_2 amplitude mode as functions of both T/T_{CDW} and x/x_c in Fig. 3 emphasizes that x-dependent mode softening—like more conventional thermal mode softening—is associated with a critical point at x_c that drives both critical softening behavior ($\omega_0 \to 0$) and overdamping of the amplitude mode as $x \to x_c$. Indeed, the x-dependent amplitude mode softening data between $0 < T \leq 100$ K, which are summarized in Fig. 4, suggest the presence of a CDW phase boundary line $x_c(T)$ in Cu_xTiSe_2 that extends—from the phase boundary line established by Morosan *et al.* [5]—to a quantum ($T \sim 0$) critical point. To obtain quantitative estimates of $x_c(T)$ in Cu_xTiSe_2 from our data, the ω_0 vs x curves in Fig. 4 were fit using the same functional form as that used to fit the x-dependent data at $T = 60$ K in Fig. 3, i.e., $\omega_0(x) = \omega_0(0)(1 - x/x_c)^\beta$ with $\beta \sim 0.15$, where $\omega_0(0)$ is the $x = 0$ value of the A_{1g} amplitude mode frequency at a particular temperature. The quantities contributing to the prefactor, $\omega_0(0)$, should not have a significant x-dependence: the reduced temperature factor in Eq. (1) varies less than 5% between $x = 0$ and $x = 0.06$, and the unscreened frequency $\tilde{\omega}$ in Eq. (1) is not expected to have a significant doping dependence in Cu_xTiSe_2 for reasons described above. Additionally, in obtaining estimates of $x_c(T)$ from our data, we assume that the scaling parameter $\beta \sim 0.15$ obtained from fits to the $T = 60$ K data in Fig. 3 does not vary significantly for the ω_0 vs x curves at the other temperatures shown in Fig. 4—this assumption is justified by the wide range of ω_0 vs T and ω_0 vs x curves that scale according the power-law form $\omega_0 \sim (1 - p)^{0.15}$ in Fig. 3 ($p = T/T_{CDW}$ or x/x_c), and by theoretical expectations [11,21]. Thus, the resulting fits of the data in Fig. 4 (solid lines) have only $x_c(T)$ as an unconstrained parameter. The estimates of $T(x_c)$ obtained from the fits in Fig. 4 are represented by the filled circles in the inset of Fig. 4; also shown for comparison are previous measurements of $T(x_c)$ (open circles) by Morosan *et al.* [5]. The reason-

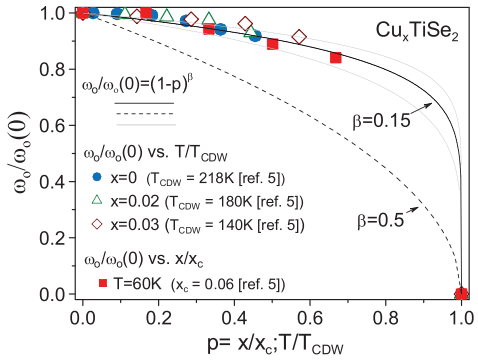

FIG. 3 (color). Plots of $\omega_0/\omega_0(0)$ vs x/x_c for $T = 60$ K ($x_c = 0.06$ [5]) (filled squares), and $\omega_0/\omega_0(0)$ vs T/T_{CDW} for $x = 0$ ($T_{CDW} = 218$ K [5]) (filled circles), $x = 0.02$ ($T_{CDW} = 180$ K [5]) (open triangles), and (iv) $x = 0.03$ ($T_{CDW} = 140$ K [5]) (open diamonds). The solid line shows that all these data sets collapse onto the same curve given by $\omega_0/\omega_0(0) = (1 - p)^\beta$, where $\beta = 0.15$ and $p = x/x_c$ or T/T_{CDW}. The gray lines provide an estimate of the uncertainty in β by comparing fits with $\beta = 0.2$ (bottom) and $\beta = 0.10$ (top). The symbol sizes represent estimated errors ($\leq$1%).

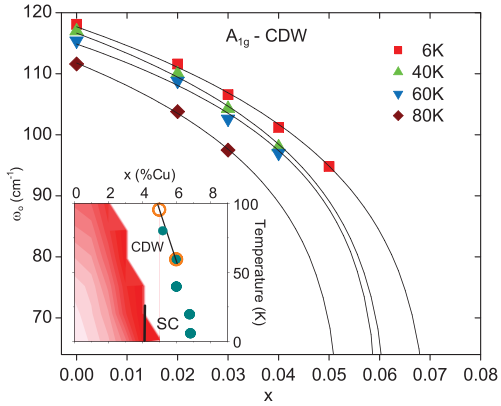

FIG. 4 (color). Summary of the A_{1g} amplitude mode frequency ω_0) vs x for different temperatures. The solid lines are fits using $\omega_0/\omega_0(0) = (1 - x/x_c(T))^{\beta}$, $w/\beta = 0.15$–0.16. (inset) Estimated values of $T(x_c)$ from the fits (filled circles); T_{CDW} data from Ref. [5] (open circles) are shown for comparison. The inset also shows a contour plot of the temperature and x-dependent linewidth Γ data, which ranges from light red ($\Gamma \sim 3$ cm^{-1}) to dark red ($\Gamma \sim 17$ cm^{-1}). The solid line denotes the superconductor (SC) phase boundary line. The symbol sizes represent estimated errors ($\leq 1\%$).

ableness of our $T(x_c)$ estimates is supported by two self-consistency checks: First, our estimates of $x_c(T)$ provide good fits of the x-dependent A_{1g} amplitude mode linewidths using the functional form, $\Gamma(T) \sim [x_c(T) - x]^{-\gamma}$ [dashed line in Fig. 2(a)], and second, our estimated value for $x_c(T = 80\ \mathrm{K})$ overlaps with the known phase boundary line from Morosan *et al.* [5].

The $T(x_c)$ values estimated from our results in Fig. 4 are consistent with a low temperature CDW phase boundary in Cu_xTiSe_2 that extends from the phase boundary line measured by Morosan *et al.* [5] down to a quantum critical point at roughly $x_c(T = 0) \sim 0.07$. This suggests that SC and fluctuating CDW order coexist in the doping range $x \sim 0.04$–0.07 of Cu_xTiSe_2. Furthermore, this result suggests that the Cu_xTiSe_2 phase diagram is consistent with Castro Neto's proposed phase diagram for the layered dichalcogenides, which has two quantum critical points as a function of increasing lattice parameter: superconductivity (SC) and CDW order coexist above the lower critical lattice parameter, while SC is present, but CDW order is not, above the higher critical lattice parameter [20]. We note, however, that because the amplitude mode becomes overdamped and unobservable very close to the transition region—due to the breakdown of long-range CDW order and zone-folding [17,18]—we cannot rule out the possibility that other effects, e.g., disorder, may lead to different quantum critical behavior (i.e., for $T \sim 0$ and near $x \sim 0.07$) than that implied by the x-dependent scaling behavior we observe up to $x = 0.05$ in Fig. 4. Consequently, it would be useful to study the putative transition region $x_c(T = 0) \sim 0.07$ with methods more sensitive to short-range, fluctuating CDW order, such as inelastic x-ray or neutron scattering. It is nevertheless interesting that the value of the quantum critical point $x_c(T = 0) \sim 0.07$ estimated from our data is close to the peak in $T_c(x)$, suggesting a possible connection between SC and fluctuating CDW order in Cu_xTiSe_2. Indeed, the inset of Fig. 4 shows a contour plot of the temperature and x-dependent A_{1g} amplitude mode linewidth, Γ, illustrating the dramatic increase of CDW fluctuations as the phase boundary is approached with increasing x and/or temperature. The connection between quantum critical behavior and the expansion of the lattice in Cu_xTiSe_2 is also suggested by pressure studies of $1T$-$TiSe_2$ [14], which show no evidence for pressure-induced $T \sim 0$ softening of the A_{1g} amplitude mode towards a quantum critical point; this suggests that pressure (lattice compression) and Cu intercalation (lattice expansion) have fundamentally different effects on the quantum phases of $1T$-$TiSe_2$.

This material is based on work supported by the U.S. Department of Energy, Division of Materials Sciences, under Grant Nos. DE-FG02-07ER46453 and DE-FG02-98-ER45706. We would like to acknowledge A. Castro Neto and M. V. Klein for useful comments.

[1] M. Imada, A. Fujimori, and Y. Tokura, Rev. Mod. Phys. **70**, 1039 (1998).
[2] N. D. Mathur *et al.*, Nature (London) **394**, 39 (1998).
[3] K. Takada *et al.*, Nature (London) **422**, 53 (2003).
[4] L. Fang *et al.*, Phys. Rev. B **72**, 014534 (2005).
[5] E. Morosan *et al.*, Nature Phys. **2**, 544 (2006).
[6] F. J. DiSalvo, D. E. Moncton, and J. V. Waszczak, Phys. Rev. B **14**, 4321 (1976).
[7] D. Qian *et al.*, Phys. Rev. Lett. **98**, 117007 (2007).
[8] J. F. Zhao *et al.*, Phys. Rev. Lett. **99**, 146401 (2007).
[9] G. Li *et al.*, Phys. Rev. Lett. **99**, 027404 (2007).
[10] M. Holt *et al.*, Phys. Rev. Lett. **86**, 3799 (2001).
[11] W. L. McMillan, Phys. Rev. B **12**, 1187 (1975); G. Gruner, *Density Waves in Solids* (Perseus Publishing, Cambridge, Massachusetts, 1994); G. Shirane, Rev. Mod. Phys. **46**, 437 (1974).
[12] M. J. Rice and S. Strassler, Solid State Commun. **13**, 1931 (1973); P. A. Lee, T. M. Rice, and P. W. Anderson, Solid State Commun. **14**, 703 (1974).
[13] E. Morosan *et al.*, Phys. Rev. B **75**, 104505 (2007).
[14] C. S. Snow *et al.*, Phys. Rev. Lett. **91**, 136402 (2003).
[15] J. A. Holy, K. C. Woo, M. V. Klein, and F. C. Brown, Phys. Rev. B **16**, 3628 (1977).
[16] N. Wakabayashi *et al.*, Solid State Commun. **28**, 923 (1978); S. S. Jaswal, Phys. Rev. B **20**, 5297 (1979).
[17] J. C. Tsang, J. E. Smith, and M. W. Shafer, Phys. Rev. Lett. **37**, 1407 (1976); G. Travaglini, I. Mörke, and P. Wachter, Solid State Commun. **45**, 289 (1983); W. K. Lee *et al.*, Phys. Rev. B **37**, 6442 (1988).
[18] W. K. Lee *et al.*, Phys. Rev. B **37**, 6442 (1988).
[19] A. Zunger and A. J. Freeman, Phys. Rev. Lett. **40**, 1155 (1978).
[20] A. H. Castro Neto, Phys. Rev. Lett. **86**, 4382 (2001).
[21] R. J. Baxter, *Exactly Solved Models in Statistical Mechanics* (Academic Press, New York, 1982).